Research Square

Preprints are preliminary reports that have not undergone peer review.
They should not be considered conclusive, used to inform clinical practice,
or referenced by the media as validated information.

Entropy-derived latent states recover pressure--volume structure in experimental intracranial hypertension

Giovanni Campanini
Consejo Nacional de Investigaciones Científicas y Técnicas
Fernando Pose
Consejo Nacional de Investigaciones Científicas y Técnicas
Carlos García
Consejo Nacional de Investigaciones Científicas y Técnicas
Nicolas Ciarrocchi
Hospital Italiano de Buenos Aires
Francisco Redelico
francisco.redelico@gmail.com

Consejo Nacional de Investigaciones Científicas y Técnicas

Article

Keywords:

Posted Date: July 29th, 2026

DOI: https://doi.org/10.21203/rs.3.rs-10019301/v1

License: This work is licensed under a Creative Commons Attribution 4.0 International License.
Read Full License

Additional Declarations: No competing interests reported.

Version of Record: A version of this preprint was published at Scientific Reports on September 15th, 2026. See the published version at https://doi.org/10.1038/s41598-026-70378-9.

Entropy-derived latent states recover pressure–volume structure in experimental intracranial hypertension

Giovanni Campanini[1], **Fernando Pose**[1], **Carlos García García**[1], **Nicolas Ciarrocchi**[2], **and Francisco O. Redelico**[1,3,*]

[1]Instituto de Medicina Translacional e Ingeniería Biomédica, CONICET – Hospital Italiano de Buenos Aires – Instituto Universitario del Hospital Italiano de Buenos Aires, Buenos Aires, Argentina
[2]Servicio de Terapia Intensiva de Adultos, Hospital Italiano de Buenos Aires, Buenos Aires, Argentina
[3]Departamento de Ciencia y Tecnología, Universidad Nacional de Quilmes, Bernal, Provincia de Buenos Aires, Argentina
[*]Corresponding author: francisco.redelico@gmail.com

ABSTRACT

Intracranial compliance determines how intracranial pressure (ICP) responds to additional intracranial volume, but the pressure–volume curve is not directly available during routine bedside monitoring. Entropy measures of the ICP waveform may carry information about this hidden mechanical state. We performed a secondary analysis of a previously published porcine model of reversible intracranial hypertension to test whether entropy-derived latent states recover experimental pressure–volume structure. ICP was acquired at 200 Hz. Normalized permutation entropy, normalized wavelet entropy and sample entropy were computed in 2 s windows with 1.5 s overlap, producing one feature vector every 0.5 s. A three-state Gaussian hidden Markov model was fitted using only entropy-derived features; absolute ICP, infused volume, pressure–volume slope and threshold labels were not model inputs. After inference, states were projected onto the ICP–volume trajectory and labelled Normal, Warning and Alert according to the corresponding pressure–volume slope. State-specific dP/dV, an inverse marker of compliance, increased across these states: 0.53, 3.84 and 7.96 mmHg ml^{-1}. Leave-one-subject-out validation yielded comparable low-, intermediate- and high-slope regimes. Thus, pressure–volume structure can be recovered from ICP waveform complexity without measuring volume or compliance directly. This preclinical proof of concept requires validation in larger experimental and clinical datasets and should not be interpreted as a clinically validated alarm system.

Introduction

Intracranial pressure (ICP) monitoring is central to neurocritical care, especially in patients at risk of intracranial hypertension after traumatic brain injury, subarachnoid haemorrhage, intracerebral haemorrhage or other acute neurological insults. Clinical management still relies heavily on mean ICP and on threshold-based decisions, commonly around 20–22 mmHg, but a single pressure value cannot fully characterize the mechanical state of the intracranial compartment[1,2]. The same ICP value may correspond to different positions on the intracranial pressure–volume curve, depending on the remaining compensatory reserve. Consequently, the clinical problem is not only to detect high ICP, but also to infer whether the intracranial system is still operating in a relatively compliant region or has moved toward a steep, low-compliance region of the pressure–volume relationship.

The pressure–volume curve provides the physiological reference for this problem. When compensatory mechanisms are preserved, an increase in intracranial volume produces only a modest pressure response. As compensatory reserve is exhausted, the curve becomes steeper and the same volume increment produces a larger pressure increase[3,4]. In this sense, the slope dP/dV is an inverse marker of compliance: larger dP/dV indicates that less additional volume is required to produce a given pressure increase. However, direct assessment of this curve requires knowledge or manipulation of intracranial volume, which is not available during routine bedside monitoring. Determining where the patient is located on the pressure–volume curve is therefore clinically meaningful, but the relevant mechanical state is hidden when only the continuous ICP waveform is available.

Information-theoretic analysis of physiological signals offers one possible route to this hidden state. The loss-of-complexity hypothesis proposes that physiological systems exhibit rich variability under preserved regulation, whereas disease, stress or loss of adaptive reserve is often accompanied by reduced or reorganized complexity[5,6]. This framework is particularly relevant to ICP because the waveform is shaped by multiple interacting mechanisms, including arterial pulsatility, venous outflow, cerebrospinal fluid dynamics, brain compliance and cerebrovascular autoregulation. A deterioration of compensatory reserve

should therefore not only change the mean pressure, but also alter the temporal organization of the ICP signal.

Several studies support this view. Approximate entropy (ApEn) analysis showed that ICP complexity decreases during acute intracranial hypertension in pediatric traumatic brain injury, suggesting disruption of the regulatory mechanisms that normally shape ICP dynamics[7,8]. Adaptive ApEn methods were later proposed for integrative analysis of heart-rate variability and ICP irregularity[9]. In adult traumatic brain injury, reduced ICP complexity has also been observed in short time series during intracranial hypertension[10]. Multiscale entropy studies extended this concept by showing that the complexity of ICP is associated with outcome after traumatic brain injury and can provide prognostic information beyond mean pressure alone[11,12]. Related work also linked early cerebrovascular signal complexity to outcome after severe traumatic brain injury[13].

Other entropy families have been applied to ICP in complementary ways. Wavelet entropy and relative wavelet entropy were used to characterize elevated ICP and suggested that intracranial hypertension is associated with redistribution of signal energy across frequency bands[14]; subsequent methodological work refined wavelet entropy estimation for ICP analysis[15]. Permutation entropy (PE), which quantifies the diversity of ordinal patterns, has been applied to ICP recordings in hydrocephalus infusion studies[16], to large clinical databases of intracranial hypertension[17], and to a porcine model of reversible intracranial hypertension[18], including a subsequent multi-entropy analysis of the same experimental framework[19]. Together, these studies indicate that entropy-based measures are sensitive to changes in ICP dynamics across experimental and clinical contexts.

The relationship between entropy and intracranial compliance has been suggested but remains incompletely established. Prior studies mainly interpreted entropy as a marker of decomplexification, intracranial hypertension, cerebrovascular dysregulation or outcome. The most direct antecedent is the porcine study by Pose et al., which reported that PE behaved inversely to ICP and that the number of missing ordinal patterns appeared to act as a surrogate of intracranial compliance[18]. However, entropy has not been systematically validated against the experimental pressure–volume curve or against state-specific dP/dV. Thus, whether entropy-derived states can recover the mechanical structure of the intracranial pressure–volume relationship remains an open question.

Entropy values alone, however, do not define physiological states. Permutation entropy captures ordinal pattern diversity, sample entropy quantifies short-term regularity, and wavelet entropy summarizes the distribution of signal energy across scales. Each descriptor emphasizes a different aspect of waveform organization. A latent-state model can integrate these complementary descriptors and provide a compact representation of the evolving physiological condition. Hidden Markov models (HMMs) are particularly suitable for this purpose because they infer unobserved states from time-dependent observations while preserving temporal continuity[20]. In the present setting, the hidden states are intended as latent representations of compliance-related intracranial dynamics. The labels Normal, Warning and Alert are therefore used as physiological vigilance labels after pressure–volume interpretation, not as clinically validated alarm categories.

The present study is a secondary computational-physiological analysis of a previously published porcine model of reversible intracranial hypertension[21]. It uses the same experimental framework as our previous entropy-based studies, but addresses a different physiological question. Earlier analyses examined the behaviour of individual entropy descriptors, missing ordinal patterns and entropy changes during intracranial hypertension[18,19]. Here, we tested whether latent states inferred from multiple entropy features can recover the experimental pressure–volume structure itself.

The key question is not whether the pressure–volume slope increases during balloon inflation; this increase is expected from intracranial physiology. The key question is whether the position of the system along that pressure–volume trajectory can be recovered from entropy-derived features of the ICP waveform alone. In the experimental setting, infused volume and dP/dV are available and can therefore be used as physiological reference variables. At the bedside, these quantities are generally unavailable. We therefore tested whether HMM states inferred only from permutation entropy, wavelet entropy and sample entropy align with regions of the pressure–volume curve with progressively increasing slope, without using absolute ICP, infused volume, pressure–volume slope or threshold labels as model inputs.

Results

Entropy features and HMM model selection

The raw ICP waveform was transformed into a sequence of entropy features computed in overlapping 2 s windows with 1.5 s overlap (Fig. 1). At each feature time, the observation vector consisted of permutation entropy, wavelet entropy and sample entropy. The HMM was fitted in this three-dimensional entropy-feature space. No absolute ICP values, infused-volume values, pressure–volume slopes, time-to-threshold labels or threshold-defined events were used as model inputs. These variables were reserved exclusively for physiological validation after state inference.

Across feature combinations, the model incorporating all three entropy measures showed the strongest likelihood-based fit. The PE–WE–SE model had the lowest AIC and BIC and the highest log-likelihood in both training and testing sets (Table 1). These results support the use of a combined entropy representation rather than a single entropy descriptor. The final model used full covariance matrices in order to allow correlations among PE, WE and SE within each latent state.

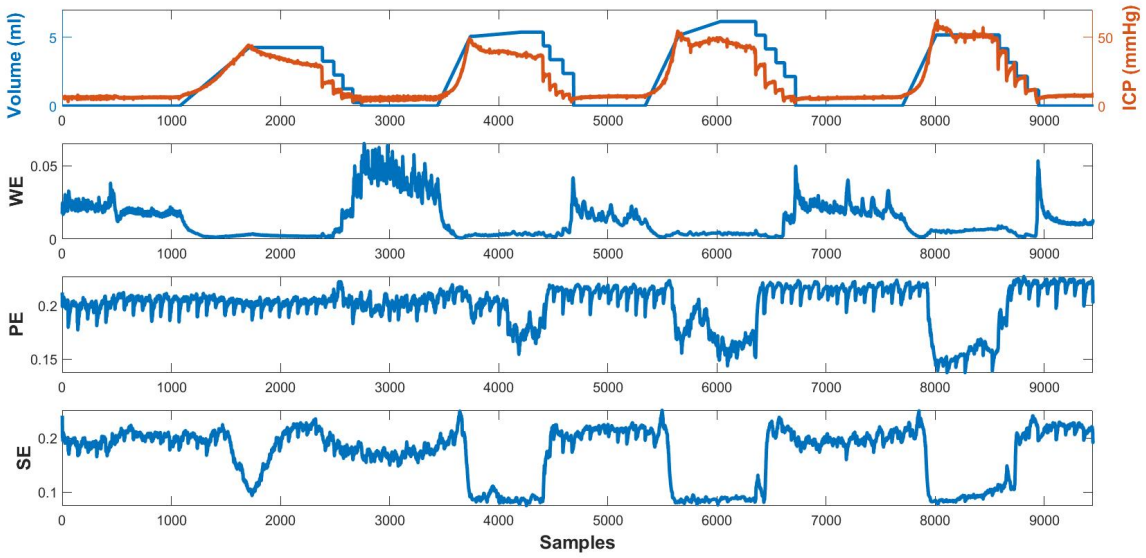


Figure 1. Representative physiological and entropy-derived time series. The upper panel shows infused volume and intracranial pressure (ICP) across consecutive experimental episodes. The lower panels show the corresponding wavelet entropy (WE), permutation entropy (PE), and sample entropy (SE), computed from the ICP waveform. These entropy-derived features constitute the observation space used by the hidden Markov model.

Table 1. Summary of entropy-feature model selection. A lower AIC/BIC and a higher log-likelihood score indicate better model fit. The model including WE, PE and SE provided the strongest likelihood-based performance and was therefore used for physiological validation.

	Training			Testing		
Entropy features	AIC	BIC	Score	AIC	BIC	Score
WE + PE + SE	-49851	-49647	24961	-49693	-49487	24881
WE + PE	-37008	-36874	18527	-35758	-35624	17902
WE + SE	-33434	-33299	16740	-33363	-33228	16704
PE + SE	-28575	-28440	14310	-26253	-26119	13150
WE	-23834	-23752	11931	-22909	-22827	11468
PE	-15819	-15737	7924	-15499	-15417	7764
SE	-13245	-13163	6637	-12716	-12634	6372

Entropy-derived states segmented the experimental episodes

Representative training and testing episodes are shown in Fig. 2. The inferred state sequence produced a structured temporal segmentation of the experimental episodes. The colour segments are interpreted in the present manuscript as entropy-derived physiological vigilance states. Normal denotes the higher-compliance portion of the pressure–volume curve, Warning denotes the transitional region, and Alert denotes the steeper low-compliance region. These labels were assigned after physiological validation and should not be interpreted as clinically validated alarm categories. This distinction is important because the HMM did not receive infused volume, pressure–volume slope or absolute ICP as inputs.

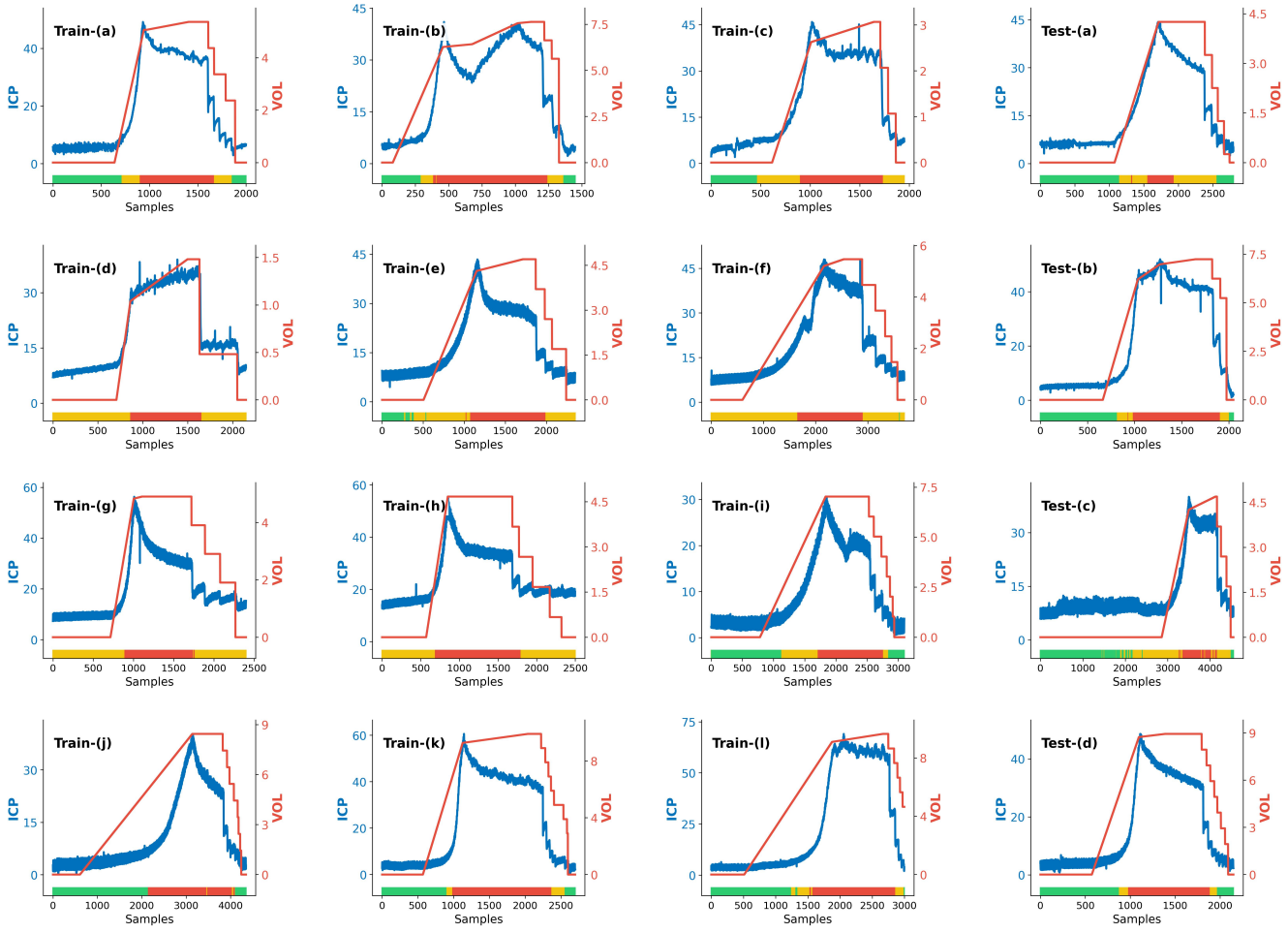


Figure 2. Representative training and testing episodes used in the analysis. For each episode, the blue trace shows intracranial pressure (ICP) and the red trace shows infused volume. The coloured bar at the bottom indicates the sequence of HMM-inferred latent states. The relevant point for the present study is that entropy-derived latent states provide a structured segmentation of the episodes without using infused volume, pressure–volume slope or absolute ICP as model inputs.

Latent states recovered ordered regions of the pressure–volume curve

When the entropy-derived states were projected onto the experimental pressure–volume trajectories, they occupied distinct regions of the curve (Fig. 3). The Normal state was associated with the flatter portion of the curve, where additional volume produced relatively small pressure changes. The Warning state occupied a transitional region. The Alert state was associated with the steepest portion of the pressure response. Importantly, this alignment was obtained only after the HMM had inferred states from entropy features alone.

The state-specific pressure–volume slope increased across the three entropy-derived states (Fig. 3 and Table 2). The median dP/dV values were 0.53 mmHg ml^{-1} for Normal, 3.84 mmHg ml^{-1} for Warning and 7.96 mmHg ml^{-1} for Alert. Bootstrap confidence intervals were [0.45, 0.60], [3.00, 4.68] and [7.59, 8.33], respectively. Since dP/dV is an inverse marker of compliance, this progression indicates that the entropy-derived states corresponded to progressively lower-compliance regions of the pressure–volume curve.

The relevant result is therefore not the expected monotonic increase of dP/dV during balloon inflation. Rather, it is that entropy-derived latent states, inferred without direct access to infused volume or pressure–volume slope, recovered regions of the experimental pressure–volume curve that are physiologically interpretable in terms of compliance.

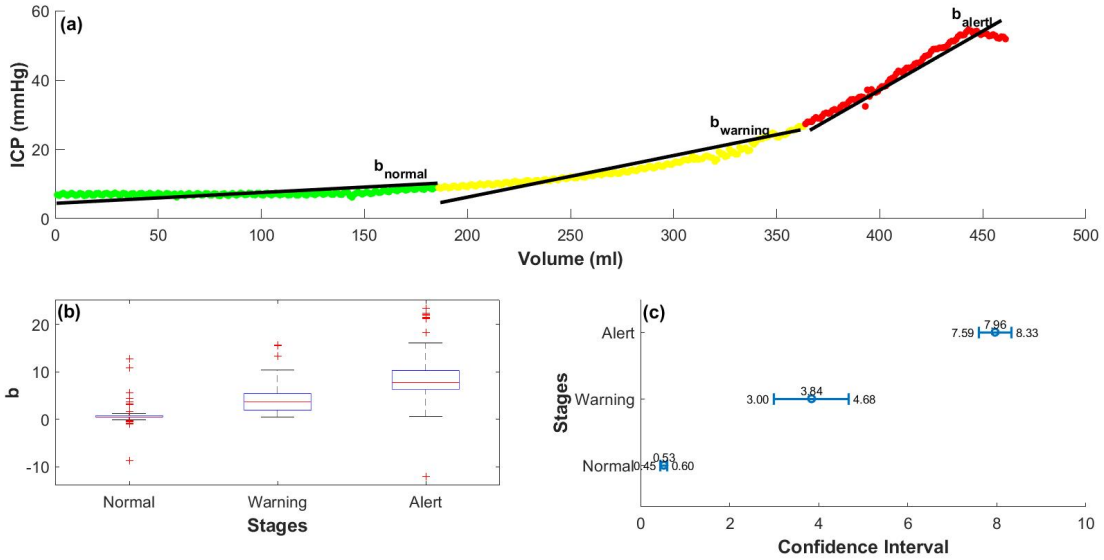


Figure 3. Physiological validation of the entropy-derived latent states against the pressure–volume relationship. (a) Representative pressure–volume trajectory coloured according to the inferred HMM states, with state-specific linear fits. (b) Distribution of state-specific pressure–volume slopes. (c) Median slope estimates with 95% confidence intervals. The labels Normal, Warning and Alert should be interpreted as entropy-derived physiological vigilance states corresponding to progressively steeper regions of the pressure–volume curve. Larger dP/dV indicates lower intracranial compliance.

Table 2. State-specific pressure–volume slopes. Slopes were estimated after HMM inference and were not used as model inputs. Labels denote physiological vigilance states derived from the post-inference pressure–volume interpretation.

State label	Median dP/dV	Bootstrap 95% CI	Physiological interpretation
Normal	0.53	0.45–0.60	Higher-compliance region
Warning	3.84	3.00–4.68	Transitional region
Alert	7.96	7.59–8.33	Lower-compliance region

Leave-one-subject-out validation preserved low-, intermediate- and high-slope regimes

To test whether the entropy-derived segmentation reflected reproducible structure across animals, we performed leave-one-subject-out (LOSO) validation. In each fold, the model was fitted using three animals and then applied to the left-out animal. State-specific pressure–volume slopes were then estimated in the held-out subject.

The LOSO analysis recovered comparable low-, intermediate- and high-slope regimes in the held-out animals (Fig. 4). The median LOSO slopes were 0.76, 4.00 and 8.75 mmHg ml^{-1} for Normal, Warning and Alert, with bootstrap intervals of [0.46, 2.17], [2.34, 4.35] and [6.46, 11.82], respectively (Table 3). These intervals were wider than those of the pooled analysis, as expected from the small number of animals, but the physiological separation between the lower-, intermediate- and higher-slope regimes remained evident. This supports the interpretation that the HMM did not merely memorize within-subject trajectories.

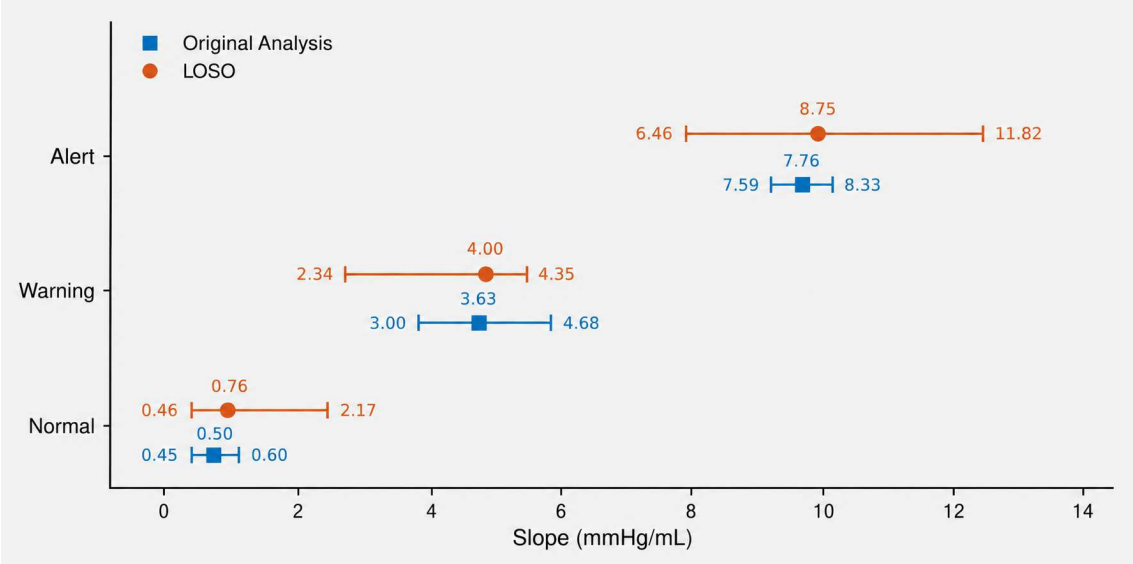


Figure 4. Leave-one-subject-out validation of pressure–volume slope regimes. The pooled analysis and the LOSO validation both recovered low-, intermediate- and high-slope dP/dV regimes corresponding to Normal, Warning and Alert. The wider LOSO intervals reflect the small number of animals, but the physiological ordering remained stable under subject-wise validation.

Table 3. LOSO validation of state-specific pressure–volume slopes. Labels denote physiological vigilance states derived from the post-inference pressure–volume interpretation.

State label	Pooled median dP/dV	LOSO median dP/dV	LOSO bootstrap 95% CI
Normal	0.53	0.76	0.46–2.17
Warning	3.84	4.00	2.34–4.35
Alert	7.96	8.75	6.46–11.82

Discussion

This study shows that entropy-derived latent states can recover physiologically meaningful regions of the intracranial pressure–volume curve in an experimental model of intracranial hypertension. The HMM was fitted using only entropy measures derived from the ICP waveform. It did not use absolute ICP, infused volume, pressure–volume slope or threshold labels as inputs. Nevertheless, when projected onto the experimental pressure–volume trajectory, the inferred states corresponded to regions of progressively increasing dP/dV. Since a steeper pressure–volume slope reflects reduced compliance, these results support the interpretation of entropy-derived states as surrogate markers of compliance-related intracranial dynamics.

The central finding should be distinguished from a trivial observation about the experimental protocol. In a balloon-inflation model, dP/dV is expected to increase as intracranial compensatory reserve is exhausted. The relevant finding is not that this increase occurs, but that the position of the system along the pressure–volume trajectory can be inferred from the ICP waveform alone through entropy-derived latent states. In the experiment, infused volume and pressure–volume slope provide the physiological reference. At the bedside, however, added intracranial volume is unknown and the pressure–volume curve cannot be computed continuously. The proposed model therefore addresses a hidden-state problem: estimating the compliance-related position of the intracranial system from continuously available signal dynamics.

The result is consistent with the broader literature on ICP decomplexification. Approximate entropy studies showed that acute intracranial hypertension is accompanied by reduced ICP complexity[7,8], and similar reductions have been reported in adult TBI using short ICP segments[10]. Multiscale entropy analyses showed that lower ICP complexity is associated with worse outcome after TBI[11,12]. Wavelet entropy studies further suggested that elevated ICP is associated not only with reduced complexity but also with redistribution of oscillatory energy across wavelet bands[14,15]. Permutation-entropy studies have reported loss of ordinal-pattern diversity during intracranial hypertension and hydrocephalus-related pressure changes[16–18]. These independent lines of evidence support the general premise that ICP waveform complexity is altered when intracranial physiology becomes mechanically or autoregulatory compromised.

The present study extends that literature by anchoring entropy-derived states to a direct mechanical reference. Previous entropy studies generally evaluated association with ICP level, intracranial hypertension episodes, hydrocephalus phases, autoregulatory status or clinical outcome. These are important endpoints, but they do not directly establish where the signal lies on the pressure–volume curve. The pressure–volume slope dP/dV provides a more direct experimental link to compliance. By showing that entropy-HMM states occupy progressively steeper regions of the pressure–volume curve, the present analysis provides a mechanistic interpretation of entropy changes: they may reflect movement of the intracranial system from a higher-compliance region to a lower-compliance region.

This distinction is important for the interpretation of entropy as a surrogate of compliance. The term surrogate should not be understood as direct measurement. Entropy does not measure compliance in physical units, and it cannot replace an experimental pressure–volume curve when volume is known. Rather, entropy may carry indirect information about the hidden mechanical state because compliance exhaustion changes the dynamic organization of the ICP waveform. The closest prior evidence for this interpretation comes from the porcine PE analysis reporting that the number of missing ordinal patterns appeared to behave as a surrogate of intracranial compliance[18]. The present study strengthens this concept by using multiple entropy features, a temporal latent-state model and explicit validation against state-specific dP/dV.

The HMM contributes by converting continuous, potentially noisy entropy fluctuations into a small number of temporally coherent states. Combining permutation entropy, wavelet entropy and sample entropy allows the model to integrate ordinal, scale-dependent and regularity-based descriptors. The model-selection results support this combined representation, with the three-entropy model showing better likelihood-based fit than single- or two-entropy alternatives. The final Gaussian HMM used full covariance matrices, allowing correlations among PE, WE and SE within each latent state. This choice is physiologically reasonable because the three entropy measures capture complementary but not independent aspects of ICP waveform organization.

The use of Gaussian emissions should be interpreted as a parsimonious working approximation in standardized entropy-feature space, not as a claim that entropy values are intrinsically Gaussian. Entropy measures may be bounded or skewed, and overlapping windows introduce temporal dependence. For this reason, classical normality tests on all feature windows are not decisive. The practical question is whether the model provides a stable and physiologically interpretable segmentation. In the present analysis, the preservation of pressure–volume slope ordering under LOSO validation suggests that the physiological interpretation is robust at the level of the available dataset. Nevertheless, future studies should compare Gaussian HMMs with transformed-feature models, mixture emissions or non-parametric state-space models.

This interpretation also clarifies how the present work differs from both prediction-oriented approaches and our previous entropy analyses of the same experimental model. The goal was not to build a forecasting model for a future ICP threshold or to compete with large-scale machine-learning models trained on heterogeneous clinical datasets. Nor was it simply to show that entropy changes during intracranial hypertension. The aim was to test whether a compact, interpretable state-space representation could recover pressure–volume structure from information-theoretic descriptors of the ICP waveform. This

distinction is important because the dataset was generated in a controlled preclinical model designed to probe intracranial mechanics, not to serve as a generic benchmark for clinical event prediction.

Several limitations should be acknowledged. First, this was a secondary analysis of a previously published preclinical dataset, not a new animal experiment or a clinical validation study. The dataset included four animals and 12 episodes, limiting statistical power and external generalizability. Second, the pressure–volume slope was estimated over an experimentally controlled interval from episode onset to the first crossing of 20 mmHg. This definition is appropriate for the experimental model but does not directly translate to clinical monitoring. Third, entropy parameters were inherited from the previous analysis pipeline and were not optimized for the present study. This avoids overfitting but requires explicit reporting of all parameter values for reproducibility. Fourth, the HMM used a compact three-state structure and Gaussian emissions; more flexible models may improve fit but could reduce interpretability. Fifth, the study does not establish that entropy-derived states can replace direct clinical assessment of intracranial compliance. It provides a proof of concept that compliance-related pressure–volume structure is encoded in ICP waveform complexity.

Despite these limitations, the result is physiologically meaningful. The experimental pressure–volume curve provides a reference that is not normally available at the bedside. The fact that entropy-derived HMM states aligned with regions of increasing dP/dV suggests that the ICP waveform contains recoverable information about the hidden mechanical state of the intracranial compartment. If validated in larger animal cohorts and human recordings, this approach may contribute to bedside neuromonitoring by providing an indirect estimate of whether the patient is likely to be located in a higher-compliance, transitional or lower-compliance region of the pressure–volume curve.

Methods

Study design

This study was designed as a secondary analysis of a previously published experimental dataset obtained in a porcine model of reversible focal intracranial hypertension[21]. No new animal experiments were performed. The aim was to evaluate whether entropy-derived latent states inferred from the ICP waveform correspond to physiologically ordered regions of the experimental pressure–volume curve.

The dataset included four animals with usable recordings. Three intracranial hypertension episodes per animal were considered, resulting in 12 episodes. Each episode consisted of controlled inflation of an intraparenchymal balloon catheter and the corresponding ICP response. The primary physiological reference was the state-specific pressure–volume slope estimated from episode onset to the first crossing of 20 mmHg.

Ethics statement

No new animal experiments were performed for the present secondary analysis. The original experimental protocol was approved by the institutional animal care committee (CICUAL, IMTIB, HIBA-IUHIBA-CONICET, protocol 0007/19). All procedures in the original study were performed in accordance with relevant institutional guidelines and regulations for animal research.

Experimental model and signal acquisition

The original experiment used healthy Landrace pigs under general anaesthesia and mechanical ventilation. Reversible focal intracranial hypertension was induced by controlled saline inflation of an intraparenchymal balloon catheter. ICP was recorded continuously using an intraparenchymal sensor, and infused volume was recorded concurrently during the balloon-inflation protocol. The raw ICP waveform was acquired at 200 Hz. Details of surgical preparation, anaesthesia, monitoring setup, data acquisition and ethical approval are provided in the original experimental report[21].

For the present analysis, the relevant signals were the raw ICP waveform and the corresponding infused-volume trajectory. The analysis interval for each episode extended from episode onset to the first time at which ICP reached 20 mmHg. This interval was selected to characterize the transition from compensated or partially compensated pressure–volume behaviour toward a conventional intracranial hypertension threshold, without using the threshold as an HMM input.

Entropy feature extraction

Let $x(t)$ denote the raw ICP waveform sampled at 200 Hz. Entropy features were computed using sliding windows of 2 s, corresponding to 400 samples per window. Consecutive windows overlapped by 1.5 s, producing one entropy-feature vector every 0.5 s. The resulting entropy-feature sequence therefore had an effective sampling rate of 2 Hz. Each feature vector was associated with the centre time of the corresponding window.

Three complementary entropy measures were computed: permutation entropy (PE), wavelet entropy (WE) and sample entropy (SE). These parameters were inherited from the previous entropy-analysis pipeline and were fixed a priori for this secondary analysis. They were not optimized to maximize the present pressure–volume result.

Permutation entropy was computed using embedding dimension $m = 5$ and delay $\tau = 1$[22]. For each windowed ICP segment $X = \{x_1, \ldots, x_N\}$, delay vectors were constructed as

$$\mathbf{x}_i^{(m)} = (x_i, x_{i+\tau}, \ldots, x_{i+(m-1)\tau}), \tag{1}$$

where $m = 5$ and $\tau = 1$. Each vector was mapped to its ordinal pattern, the empirical distribution $p(\pi)$ of ordinal patterns was estimated within the window, and PE was computed as

$$H_{PE} = -\sum_{\pi} p(\pi) \log p(\pi). \tag{2}$$

The reported PE feature was normalized by the maximum entropy $\log(m!)$.

Wavelet entropy was computed using a discrete wavelet transform with a Daubechies-4 mother wavelet and six decomposition levels. For each window, the ICP segment was decomposed into subbands including the detail coefficients and the final approximation coefficients. The energy of each retained subband was computed and converted into relative energy,

$$P_j = \frac{E_j}{\sum_{k=1}^{J} E_k}, \tag{3}$$

where E_j is the energy of the jth subband and J is the number of retained subbands. WE was then calculated as

$$H_{WE} = -\sum_{j=1}^{J} P_j \log P_j. \tag{4}$$

The reported WE feature was normalized by the maximum entropy $\log(J)$.

Sample entropy was computed as a measure of short-term regularity[23]. Template vectors of length $m_{SE} = 2$ were compared using the Chebyshev distance. The tolerance parameter was set to $r_{SE} = 0.2\sigma$, where σ denotes the standard deviation of the windowed ICP segment. SE was computed as

$$H_{SE}(m_{SE}, r_{SE}, N) = -\log \frac{A(m_{SE}+1, r_{SE})}{B(m_{SE}, r_{SE})}, \tag{5}$$

where B is the number of matching vector pairs of length m_{SE} within tolerance r_{SE} and A is the corresponding number for length $m_{SE}+1$. After entropy extraction, all three features were standardized before HMM fitting.

Hidden Markov modelling

At each feature time t, the observation vector was defined as

$$\mathbf{z}_t = [H_{PE}(t), H_{WE}(t), H_{SE}(t)]^{\top}. \tag{6}$$

Only entropy-derived features were used as HMM observations. Absolute ICP, infused volume, time from episode onset, pressure–volume slope and threshold labels were excluded from the model inputs.

A three-state Gaussian HMM was implemented in Python using `hmmlearn` and fitted to the entropy-feature sequences[20]. The number of states was chosen a priori as a minimal interpretable representation of the pressure–volume transition. Episodes were treated as separate sequences and were not considered a single continuous recording. The emission distribution for each hidden state was modelled as a multivariate Gaussian distribution with a full covariance matrix,

$$\mathbf{z}_t \mid q_t = s \sim \mathcal{N}(\mu_s, \Sigma_s), \tag{7}$$

where q_t is the latent state, μ_s is the state-specific mean vector and Σ_s is the state-specific covariance matrix. Full covariance matrices were used to allow correlations among PE, WE and SE within each latent state.

Entropy features were standardized before model fitting. In LOSO validation, standardization parameters were estimated only from the training animals and then applied to the left-out animal. The Gaussian emission model was used as a parsimonious working approximation in standardized feature space. It was not interpreted as a claim that entropy values are intrinsically Gaussian. The adequacy of the model was evaluated by likelihood-based model selection, physiological interpretability of the inferred states and subject-wise preservation of the low-, intermediate- and high-slope pressure–volume regimes.

Because HMM state labels are arbitrary, labels were assigned after inference according to the median pressure–volume slope associated with each state. The lowest-slope state was labelled Normal, the intermediate-slope state was labelled Warning and the highest-slope state was labelled Alert. These labels were not used during HMM training and should be interpreted as physiological vigilance labels derived from post-inference pressure–volume analysis, not as clinically validated alarm categories.

Pressure–volume slope

The physiological validation of the entropy-derived states was based on the experimental pressure–volume relationship. For each episode, infused volume V was placed on the horizontal axis and ICP P on the vertical axis. The pressure–volume slope was expressed as dP/dV in mmHg ml^{-1}.

For each episode and each HMM state, all points assigned to that state within the analysis interval were extracted. A linear model was fitted as

$$P_i = \alpha_s + \beta_s V_i + \varepsilon_i, \quad i \in I_s, \tag{8}$$

where I_s is the set of points assigned to state s, α_s is the state-specific intercept and β_s is the state-specific pressure–volume slope. Since compliance is related to dV/dP, a larger $\beta_s = \mathrm{dP}/\mathrm{dV}$ was interpreted as lower compliance. Slopes were not used as HMM inputs; they were used only after inference as physiological reference values.

Leave-one-subject-out validation

To assess whether the entropy-derived segmentation reflected reproducible physiological structure across animals, leave-one-subject-out validation was performed. In each fold, one animal was held out, the HMM was fitted using the remaining animals, and the trained model was applied to the left-out animal. State-specific pressure–volume slopes were then estimated in the held-out animal. Because only four animals were available, LOSO was interpreted as a conservative robustness analysis rather than a fully powered external validation.

Statistical analysis

Continuous variables were summarized using medians, interquartile ranges, means and standard deviations as appropriate. Bootstrap confidence intervals were used to quantify uncertainty in state-specific median slopes. For each state, 10,000 bootstrap resamples of episode-level slopes were generated, and 95% confidence intervals were computed using the 2.5th and 97.5th percentiles of the bootstrap distribution. The main physiological criterion was recovery of distinct low-, intermediate- and high-slope pressure–volume regimes across entropy-derived states. Statistical analyses were performed in Python.

Data availability

The source data supporting the findings of this study derive from the original animal experiment and are available from the corresponding author upon reasonable request, subject to institutional and ethical restrictions related to the original experimental protocol. The analysis code used for the present secondary analysis is available from the corresponding author upon reasonable request.

Acknowledgements

The authors thank the clinical, veterinary and technical teams involved in the original experimental protocol.

Author contributions statement

G.C., F.P., C.G.G. and F.O.R. contributed to the conception and design of the analysis. N.C. contributed to the original experimental model and physiological interpretation. G.C. and F.P. performed the computational analysis. G.C., F.P. and F.O.R. prepared the figures and tables. F.O.R. supervised the study and drafted the manuscript. All authors contributed to interpretation of the results, critically revised the manuscript and approved the final version.

Competing interests

The authors declare no competing interests.

Funding

No specific funding was received for the present secondary analysis.

References

1. Carney, N. et al. Guidelines for the management of severe traumatic brain injury, fourth edition. *Neurosurgery* **80**, 6–15; 10.1227/NEU.0000000000001432 (2017).

2. Czosnyka, M. & Pickard, J. D. Monitoring and interpretation of intracranial pressure. *J. Neurol. Neurosurg. Psychiatry* **75**, 813–821; 10.1136/jnnp.2003.033126 (2004).

3. Marmarou, A., Shulman, K. & Rosende, R. M. A nonlinear analysis of the cerebrospinal fluid system and intracranial pressure dynamics. *J. Neurosurg.* **48**, 332–344; 10.3171/jns.1978.48.3.0332 (1978).

4. Avezaat, C. J. J. & van Eijndhoven, J. H. M. Intracranial pressure and pressure-volume relationships. *J. Neurosurg.* **61**, 1117–1124; 10.3171/jns.1984.61.6.1117 (1984).

5. Lipsitz, L. A. & Goldberger, A. L. Loss of complexity and aging: potential applications of fractals and chaos theory to senescence. *JAMA* **267**, 1806–1809 (1992).

6. Goldberger, A. L. et al. Fractal dynamics in physiology: alterations with disease and aging. *Proc. Natl Acad. Sci. USA* **99**, 2466–2472; 10.1073/pnas.012579499 (2002).

7. Hornero, R., Aboy, M., Abasolo, D., McNames, J. & Goldstein, B. Interpretation of approximate entropy: analysis of intracranial pressure approximate entropy during acute intracranial hypertension. *IEEE Trans. Biomed. Eng.* **52**, 1671–1680; 10.1109/TBME.2005.855722 (2005).

8. Hornero, R., Aboy, M., Abasolo, D., McNames, J., Wakeland, W. & Goldstein, B. Complex analysis of intracranial hypertension using approximate entropy. *Crit. Care Med.* **34**, 87–95; 10.1097/01.CCM.0000190426.44782.F0 (2006).

9. Hu, X., Miller, C., Vespa, P. & Bergsneider, M. Adaptive computation of approximate entropy and its application in integrative analysis of irregularity of heart rate variability and intracranial pressure signals. *Med. Eng. Phys.* **30**, 631–639; 10.1016/j.medengphy.2007.07.002 (2008).

10. Soehle, M., Gies, B., Smielewski, P. & Czosnyka, M. Reduced complexity of intracranial pressure observed in short time series of intracranial hypertension following traumatic brain injury in adults. *J. Clin. Monit. Comput.* **27**, 395–403; 10.1007/s10877-012-9427-0 (2013).

11. Lu, C.-W. et al. Complexity of intracranial pressure correlates with outcome after traumatic brain injury. *Brain* **135**, 2399–2408; 10.1093/brain/aws155 (2012).

12. Zeiler, F. A. et al. Association between physiological signal complexity and outcomes in moderate and severe traumatic brain injury: a CENTER-TBI exploratory analysis of multi-scale entropy. *J. Neurotrauma* **38**, 272–282; 10.1089/neu.2020.7249 (2021).

13. Gao, L., Smielewski, P., Czosnyka, M. & Ercole, A. Cerebrovascular signal complexity six hours after intensive care unit admission correlates with outcome after severe traumatic brain injury. *J. Neurotrauma* **33**, 2011–2018; 10.1089/neu.2015.4228 (2016).

14. Xu, P., Scalzo, F., Bergsneider, M., Vespa, P., Miller, C. & Hu, X. Wavelet entropy characterization of elevated intracranial pressure. *Conf. Proc. IEEE Eng. Med. Biol. Soc.* **2008**, 2924–2927; 10.1109/IEMBS.2008.4649815 (2008).

15. Xu, P., Hu, X. & Yao, D. Improved wavelet entropy calculation with window functions and its preliminary application to study intracranial pressure. *Comput. Biol. Med.* **43**, 425–433; 10.1016/j.compbiomed.2013.01.022 (2013).

16. Adjei, T., Abasolo, D. & Santamarta, D. Intracranial pressure for the characterization of different types of hydrocephalus: a permutation entropy study. *Conf. Proc. IEEE Eng. Med. Biol. Soc.* **2015**, 4198–4201; 10.1109/EMBC.2015.7319320 (2015).

17. Ciarrocchi, N., Quiroz, N., Traversaro, F., San Roman, E., Risk, M., Goldemberg, F. & Redelico, F. O. The complexity of intracranial pressure as an indicator of cerebral autoregulation. *Commun. Nonlinear Sci. Numer. Simul.* **75**, 192–199; 10.1016/j.cnsns.2019.03.018 (2019).

18. Pose, F., Ciarrocchi, N., Videla, C. & Redelico, F. O. Permutation entropy analysis to intracranial hypertension from a porcine model. *Entropy* **25**, 267; 10.3390/e25020267 (2023).

19. Pose, F., Videla, C., Campanini, G., Ciarrocchi, N. & Redelico, F. O. Using entropies to monitoring intracranial pressure, evidence from an animal model. *Biomed. Signal Process. Control* **86**, 105320; 10.1016/j.bspc.2023.105320 (2023).

20. Rabiner, L. R. A tutorial on hidden Markov models and selected applications in speech recognition. *Proc. IEEE* **77**, 257–286; 10.1109/5.18626 (1989).

21. Ciarrocchi, N. M. et al. Reversible focal intracranial hypertension swine model with continuous multimodal neuromonitoring. *J. Neurosci. Methods* **373**, 109561; 10.1016/j.jneumeth.2022.109561 (2022).

22. Bandt, C. & Pompe, B. Permutation entropy: a natural complexity measure for time series. *Phys. Rev. Lett.* **88**, 174102; 10.1103/PhysRevLett.88.174102 (2002).

23. Richman, J. S. & Moorman, J. R. Physiological time-series analysis using approximate entropy and sample entropy. *Am. J. Physiol. Heart Circ. Physiol.* **278**, H2039–H2049; 10.1152/ajpheart.2000.278.6.H2039 (2000).

Supplementary Files

This is a list of supplementary files associated with this preprint. Click to download.

- stream.jpg